Automatic Generation Control Using an Energy Storage System in a Wind Park

Tapabrata Chakraborty, David Watson, and Marianne Rodgers

***Abstract*—This paper demonstrates the operation of a 1 MW/2 MWh grid-tied battery energy storage system (BESS) in a 10 MW wind R&D park for Automatic Generation Control (AGC) for 29 days. The efficiency and utilization of the BESS in the context of regulation and grid integration are examined. The response time for the BESS is as low as one second, which is faster than the current accepted practice of a conventional generator with governor control. Using PJM's performance template gives an average performance score of 93% while the storage is providing AGC. However, because the storage system only charges when there is sufficient wind energy and spent significant time in maintenance mode, the 29-day performance average is only 65%. The battery was able to carry out some mode of AGC for 64% of the test period. When energy costs and battery degradation are considered, utilizing the battery costs USD 19,000 over the 29-day period, whereas the potential income from AGC, charging only with wind power, was USD 9,037. This 29-day demonstration shows that batteries have fast response and can perform AGC, but within a wind farm AGC is unlikely to be suitable without changes in the tariff schemes.**

***Index Terms*—Energy storage (batteries), power system, regulation, wind energy integration.**

I. Introduction

In RECENT years, there has been an increase in penetration of renewable energy, which involves major challenges in grid stability, reliability and security [1]. Renewable energy resources such as wind and solar are intermittent, which makes them non-dispatchable energy resources. Due to the fluctuating nature of renewable energy resources, there is a necessity for smart, fast, and reliable technology for grid integration. Moreover, while conventional generating units provide regulation to ensure that frequency does not deviate significantly during large transient events, renewable energy technologies often do not have these capabilities, or do not use them for economic reasons. As penetration of intermittent renewable generation increases and conventional thermal plants with regulation capabilities are displaced, there is concern that there will be a decline in frequency regulation and dispatchable generation on the grid [2], [3].

One way to deal with these issues is through a Battery Energy Storage System (BESS). A BESS converts intermittent renewable energy into dispatchable energy to help control electrical demand. Furthermore, a BESS can be ramped up or down in a relatively short amount of time, which increases the ability to control the grid frequency. A BESS can also be used to store surplus energy produced during curtailments and supply power during high demand. Energy storage can make grid networks more reliable in the context of generation and demand balance. The response time for energy storage performing Automatic Generation Control (AGC, also known as load frequency control) can be as little as one to two seconds, unlike gas turbines, which have response times in minutes [4]. Compared to conventional generators that are integrated to the electrical grid as generation and ancillary services, energy storage has undergone a remarkable evolution over the past few years. It has unlocked a new era of possibilities to provide grid reliability as the electricity network continues to evolve.

AGC is one type of regulation and is typically responsible for restoring the grid frequency to its nominal value. As a result, it will decrease the Area Control Error (ACE), ensuring that frequency and interchange energy schedules between regional balancing authorities are followed. Under normal conditions, the electrical grid frequency fluctuates bi-directionally around the nominal system frequency. Conventional fossil fuel power plants, which are set at an intermediate output, are used to change their output power to maintain the grid's stability. Since energy storage systems can absorb as well as inject power into the grid, they can effectively double their capacity range, compared to a conventional generator that can only produce electricity, and cannot absorb it. Furthermore, conventional turbines have a gradual ramp up or down, whereas energy storage can ramp up or down from idle to full rated charge or discharge within seconds. This attribute increases the transient stability of the system [6].

Frequency response has been investigated in the Eastern interconnected area and it has been determined that governor response from wind plants can provide significant frequency response. However, the curtailment to provide this service represents a substantial opportunity cost to wind plant owners [7]. Storage providing this service could avoid this cost as demonstrated in the Western area integration study where it was shown that about 400 MW of storage could ensure that all areas met their frequency response obligation [8].

Manuscript received June 8, 2016; revised October 16, 2016 and March 26, 2017; accepted April 29, 2017. Date of publication May 8, 2017; date of current version December 20, 2017. This work was supported by the Natural Resources Canada's Clean Energy Fund. Paper no. TPWRS-00873-2016. *(Corresponding author: Marianne Rodgers.)*

T. Chakraborty is with the Wind Energy Institute of Canada, North Cape, PE C0B 2B0, Canada, and also with the University of Regina, Regina, SK S4S 0A2, Canada (e-mail:tapabrata.chak@gmail.com).

D. Watson and M. Rodgers are with the Wind Energy Institute of Canada, North Cape, PE C0B 2B0, Canada (e-mail:david.watson@weican.ca; marianne.rodgers@weican.ca).

Color versions of one or more of the figures in this paper are available online at http://ieeexplore.ieee.org.

Digital Object Identifier 10.1109/TPWRS.2017.2702102

Xu *et al.* [9] simulated control strategies aimed at maintaining a BESS's state of charge in AGC applications in two different regulation markets. They proposed using the intraday market so the BESS can be recharged without disturbing its operation. By modeling the degradation and other cost factors, they determined that the flexible PJM network was more profitable than the German network, mainly due to higher reserve capacity payments in the PJM market [9].

Lietermann [10] proposes splitting the regulation burden into two sections, one provided by fast responding units and the other by traditional generators. This has been carried out in PJM, creating the Reg A signal for traditional generators and the Reg D signal, which is energy neutral, for fast responding units such as energy storage.

Examples of storage providing regulation are becoming increasingly common [11]–[13], and demonstrate the fast response of the BESSs. However, real world issues such as maintenance, efficiency, and financial cost/benefits while providing AGC with a battery have not been addressed in detail. It is important to understand the issues that can occur when deploying a battery in an actual grid-connected environment, before there can be widespread acceptance of the BESS technologies as well as appropriate development of markets for the services they offer. This paper will analyze the results in terms of accuracy and efficiency of a grid-connected battery performing AGC in the context of a wind park where only wind power is used to charge the battery. Additionally, the economic implications in the PJM market will be compared to the cost to the storage system owner/operator.

The purpose of this paper is to demonstrate the implementation of energy storage to perform AGC in a grid-connected wind park and to explore the performance and drawbacks as discovered through the implementation of the control strategy. The behavior of a 1 MW/2 MWh battery in a 10 MW Wind R&D Park located in Prince Edward Island, Canada is analyzed with the following objectives:

1) Create and demonstrate controls for the use of a grid connected BESS for AGC utilizing wind power
2) Calculate battery efficiency and accuracy
3) Calculate the financial costs and benefits of utilizing storage for AGC in a relevant jurisdiction.
4) Examine the implications of real world testing that are typically not considered in simulations

Most jurisdictions do not offer compensation for the benefits that energy storage can offer. By carrying out and publishing results from real world demonstrations such as in this paper, the benefits will be realized by utilities and system operators and markets will develop.

II. Overview of Wind Park Control System

A. Wind R&D Park

The Wind R&D Park consists of five DeWind D9.2 wind turbines capable of providing a total of 10 MW, as well as GE's 2 MWh Durathon battery interfaced by S&C's 1 MW Purewave Inverter.

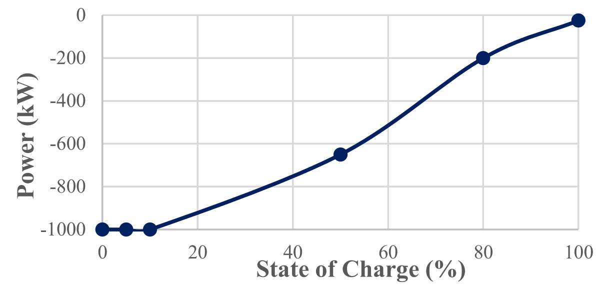

Fig. 1. Theoretical charge profile for Durathon battery [20].

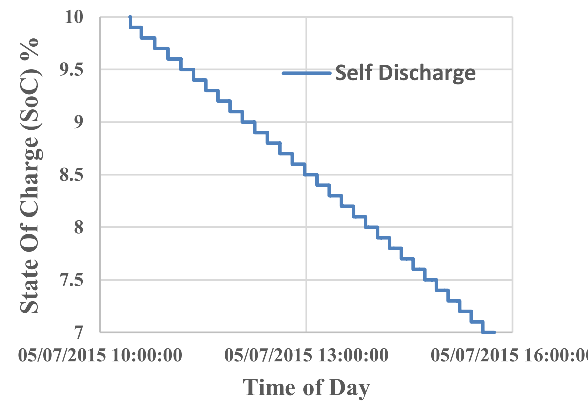

Fig. 2. Self-discharge characteristics of the battery.

The battery charge profile designates the magnitude of power acceptance by the battery at different states of charge. The theoretical battery charge profile for the Durathon battery is shown in Fig. 1. As the state of charge (SoC) increases for this battery, the magnitude of power the battery can accept decreases. The theoretical discharge profile is 1 MW from 100% to 10%, decreases linearly to 0 MW at 0%.

Although GE Durathon batteries have a high energy density, they also have a high self-discharge rate when idle due to having an operating temperature of 280 °C. Fig. 2 shows self-discharge characteristics of the battery. The battery loses 1% SoC every two hours.

III. Automatic Generation Control Methodology

A. Battery Operation

In this experiment, because real time AGC data was not available, historic reg. D PJM AGC data was used to represent the performance of the storage system under utility control. In future work real time frequency measurements or real time AGC signals could be used.

The normal AGC operation was constrained to when there was sufficient wind power (greater than 1 MW) from the 10 MW Wind R&D Park. This constraint guarantees zero demand charge during battery operation and ensures all absorbed energy is from the wind turbines. The demand charge by the local utility at the wind R&D park was USD 5.72/kW in July 2014 for the highest 15 minute period in the month, therefore the cost of a 1 MW charging period (down-regulation) with no wind power would have been USD 5,720, which was not financially viable. Having

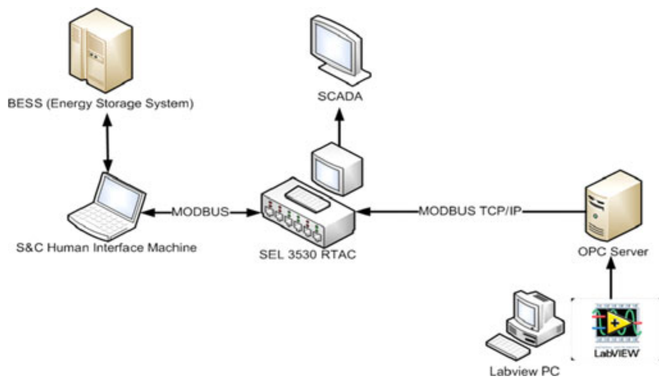

Fig. 3. Schematic for LabVIEW and Modbus network.

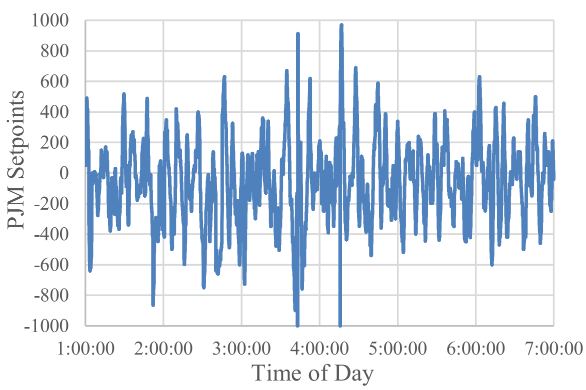

Fig. 4. PJM data for automatic generation control for six hours on July 1.

the battery on-site with wind power does not affect its accuracy to provide AGC, but does affect the amount of time it can provide AGC due to the financial constraint of the demand charge, Co-location of storage and wind is not necessarily beneficial for AGC but can be beneficial for other services.

For AGC, the battery was controlled under two modes of operation: Setpoint Mode and Maintenance Mode. The BESS toggled between operational modes depending upon the maintenance cycle request, which was controlled by the GE storage system and was requested weekly.

1) AGC User Logic (Setpoint Mode): In Automatic Generation Control, the battery receives an AGC setpoint every four seconds and delivers the positive or negative power. This allows the battery to behave as a fast responding unit to decrease the balancing area control error.

The power setpoint to control the battery charging (negative power, down-regulation) and discharging (positive power, up-regulation) was sent from the Labview PC to the BESS over the Modbus Network as shown in Fig. 3. A Modbus I/O server on a host computer served as a master to communicate with the slave using Modbus protocol.

Twenty-nine days of historic PJM data from August 2013 was used to test the battery's response to grid automatic generation control. Fig. 4 shows six hours of this data from July 1, 2015 as a representation of the type and range of data used. A LabVIEW program with user logic, which enabled the user to start the program at any time of day was implemented. It generated an index based upon the hour, minute, and second of the day. At

TABLE I
CONDITIONS FOR THE OPERATING MODES

Operating Mode	Condition
Maintenance Cycle	When requested by BESS and wind power is greater than 2 MW. Controls end maintenance cycle if wind power is less than 500 kW
Automatic Generation Control (Up and Down Regulation)	State of Charge (SoC) between 10% to 90% and wind power above 1 MW
Automatic Generation Control (Down-Regulation)	SoC less than 10% and wind power above 1 MW
Automatic Generation Control (Up-Regulation)	SoC greater than 90% or SoC between 10% to 90% and wind power less than 1 MW
Idle	SoC less than 10% and wind power less than 1 MW or maintenance cycle required and wind power lower than required

the start of each day the program synchronized with the satellite clock.

The user logic was incorporated in RTAC using IEC 61131-3 ST (Structured-Text) program. The operating modes for the study were classified into five categories, as shown in Table I. In Table I the condition describes the circumstances under which the battery would be operating in each operation mode, which is dependent upon the SoC and wind power constraints.

A server Modbus protocol was used to communicate between the RTAC and the LabVIEW OPC server. The setpoint is converted into a 16 bit integer and mapped to a holding register in RTAC. Although there is a delay in SCADA communication, it is insignificant in this context. The response time for the BESS is as low as one second, which, when compared to a conventional generator with governor control, is a better reaction than the current accepted practice. As BESSs are interfaced to the grid through power electronics, they do not contribute to the momentum on the grid, although their fast response time makes them an appropriate device to help arrest sharp changes in system frequency.

The frequency with which each power output was requested by the PJM signal is shown in Fig. 5. A bell curve shows the normal distribution of the PJM data. It can be seen from Fig. 5 that the histogram is shifted slightly towards the left. Because the BESS's efficiency is not 100%, the battery does not reach its original SoC from an equal charge-discharge cycle. Therefore, a –30 kW offset was added to the PJM data as this is the BESS's nominal power.

2) Maintenance Mode Operation: GE Durathon batteries require a maintenance cycle after every 168 h of operation. During the maintenance cycle, the Multi-Battery Manager (MBM) ensures that all the modules in the BESS reach 100% SoC. Typically, the maintenance cycle takes 12 to 13 hours. During the maintenance cycle, the battery is unavailable, although the maintenance cycle can be interrupted if the battery is required. Battery characteristics during a maintenance cycle are shown in Fig. 6. During a maintenance cycle, the battery performs several

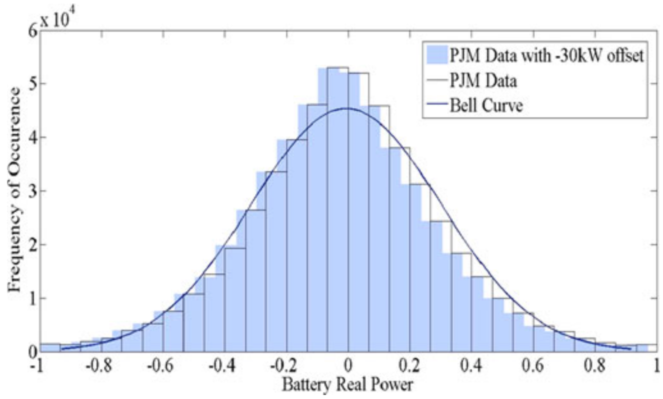

Fig. 5. Distribution of PJM data.

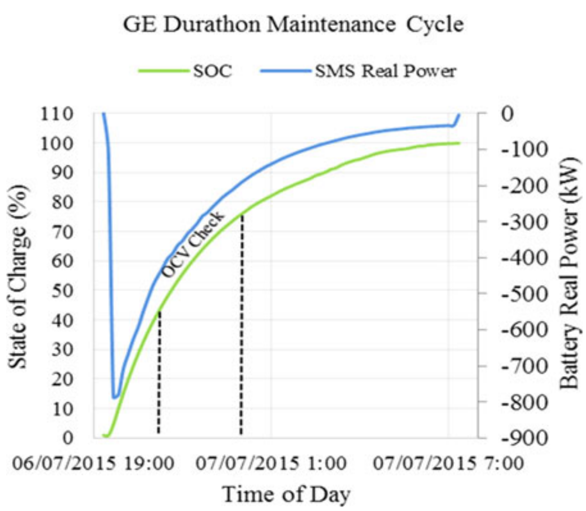

Fig. 6. Battery characteristics during maintenance cycle.

operations including open circuit voltage checks to check the health of the battery and a top of charge to reset the SoC value. The maintenance cycle ends when top of charge is reached.

B. Cost/Benefits Calculations

The Federal Energy Regulatory Commission (FERC) regulates the sale of electricity in the United States. The FERC01 reliability standard rewards fast acting resources for providing faster regulation to system operators. This generates revenue for fast-acting resources and decrease frequency response time of the system. FERC orders 755 and 784 increased the revenue for resources with superior response and accuracy, which enables technologies like flow batteries and flywheels to participate in the grid ancillary services market.

For this study, the benefits provided by the PJM are used to calculate the potential benefits the battery could have earned through the study. The payment in the PJM market comprises two parts, with the performance payment weighted by a performance score:

a) *Capability Payment*

b) *Performance Payment*

The method to calculate the payments can be found in the performance score template from PJM [21], [22]. The capability component (*RegCapabilityPriceCredit*) is a function of the regulation market capability clearing price (*RegCapabilityPrice*$_t$):

$$Reg\,Capability\,Price\;\;Credit = REG_t \cdot n_t \cdot Reg\,Capability\,Price_t \qquad (1)$$

Where REG_t is the hourly integrated regulation and n_t is the actual performance score for the hourly period.

For fast responding resources, the performance component (*RegPerformancePrice Credit*) is a function of the regulation market performance clearing price (*RegPerformancePrice*):

$$Reg\,Performance\,Price\;\;Credit = REG_t \cdot n_t \cdot mileage\,ratio \cdot Reg\,Performance\,Price \qquad (2)$$

The performance score (n_t) is averaged over a five minute period for each ten second set of calculations and PJM will determine a composite Performance Score per resource as a unitless scalar ranging from 0 to 1. The Performance Score is a weighted average of the performance score components:

$$n_t = A\,(delay\;score) + B\,(accuracy\;score) + C\,(precision\;score) \qquad (3)$$

The component scalars (*A*, *B*, and *C*) may range from 0 to 1, but must total to 1, and in PJM are currently rated equally (0.33), which means the performance score is the average of the accuracy score, delay score, and precision score.

The *Delay Score* is calculated for each ten second interval starting from Time 0 + 10 to quantify the delay in response between the AGC signal and the resource change in output. The match is calculated using the statistical correlation function, *r*, which measures the degree of relationship between the two signals. By shifting the time periods to compare the signals, delay (δ) is defined at the point in time of the maximum correlation between the two signals. This also results in an *Accuracy Score*:

$$Accuracy\,Score = \max_{\delta=0\;to\;5\;\mathrm{min}} r_{Signal\;Response}\,(\delta, \delta + 5\;\mathrm{min}) \qquad (4)$$

$$Delay\;Score = Abs\left(\frac{5\,\mathrm{min} - \delta}{5\,\mathrm{min}}\right) \qquad (5)$$

The precision score is calculated for each ten second interval starting from Time 0 + 10 as a function of the difference in the energy provided versus the energy requested by the AGC signal while scaling for the number of samples. Each ten second sample is averaged over an hourly basis and PJM calculates the *Precision Score* as the absolute error as a function of the resource's regulation capacity:

$$Error = Average\;of\;\;Abs \times \left(\frac{Response - Regulation\;Signal}{Hourly\;Average\;Regulation\;Signal}\right)$$

$$Precision\;Score = 1 - \frac{1}{n}\sum Abs\,(Error) \qquad (6)$$

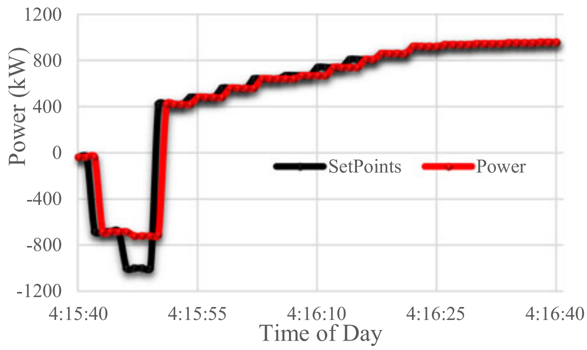

Fig. 7. Battery characteristics during ramp up.

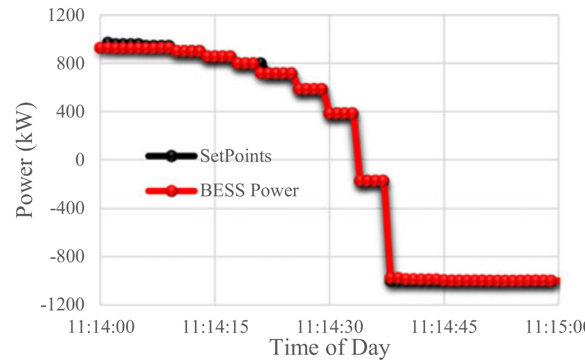

Fig. 8. Battery characteristics during ramp down.

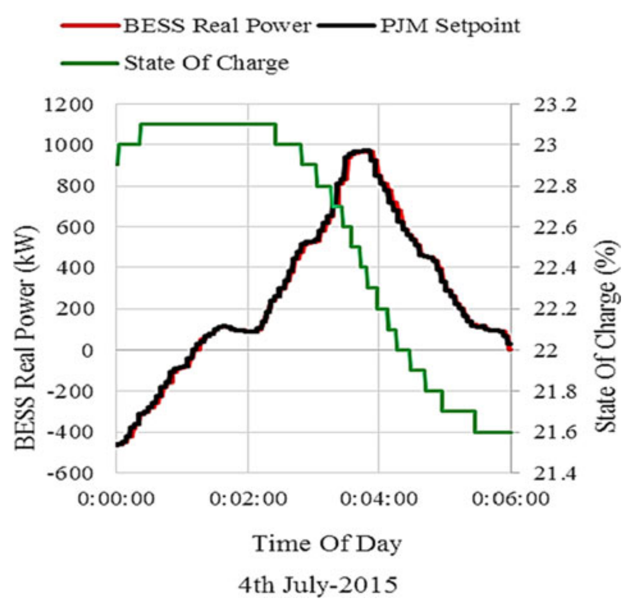

Fig. 9. Example of battery operation.

Where n is the number of samples in the hour and the precision allows ten seconds for signal propagation delay for regulating resources.

Mileage is the absolute sum of movement of the AGC signal in a given time period:

$$Mileage = \sum\nolimits_{t=0}^{n} |RegD_t - RegD_{t-1}| \quad (7)$$

The *Mileage Ratio* is a measure of the relative work of Regulation D (for faster responding resources) resources relative to Regulation A (for traditional regulating resources):

$$Mileage\ Ratio = \frac{Mileage_{RegA}}{Mileage_{RegD}} \quad (8)$$

The financial results in the present scenario are analysed using PJM regulation prices from July 2015. For the financial analysis, the mileage ratio from July 2015 was used rather than the mileage of the signal (which was from 2013). To get the revenue (1) and (2) are summed for each hour that the battery provided AGC.

The cost of performing AGC is based on the lost energy due to the inefficiency of the inverter/battery and the lifetime reduction of the system. The lifetime of the storage system and inverter is estimated to be 4,500 cycles or 10 years by the manufacturer [16], [20]. It is assumed that a cycle is 1600 kWh (80% depth of discharge).

IV. Results and Discussion

In this work, the capabilities of an energy storage system to perform AGC in a Wind R&D Park were evaluated. During normal AGC, the BESS ramps up and ramps down the power in accordance with the PJM setpoints. For a significant portion of the time, the battery was capable of following the setpoints. Ramp rates are typically $<$50 kW/s but ramp-up rates as high as $1.13\,\mathrm{MW/s}$ were observed with the BESS's output power changing from –710 kW to 420 kW within one second. As shown in Fig. 7, the setpoint changes from –1000 kW to 421 kW and then continues to climb to 966 kW. Due to the BESS having a SoC of 63% at this time, the BESS was unable to respond accurately to the –1000 kW setpoint as was noted in Fig. 1. This shows that the ramp rate of the battery did not limit the accuracy at which the battery responded to the setpoint.

Similarly, ramp-down rates of 0.81 MW/s were observed with the output changing from –171 kW to –976 kW within one second, and the BESS output ranging from 926 kW to –1000 kW in under a minute, as shown in Fig. 8. The SoC at the time was 12%, allowing for –1000 kW to be reached. Fig. 9 shows a typical period in AGC where the battery ramps up to 1 MW output within two minutes.

However, in some cases the battery could not accurately follow the setpoints. Fig. 10 shows the average difference between setpoint and actual power output of the battery when charging and discharging during automatic generation control as a function of SoC. As shown in Fig. 10, the error is higher as the SoC increases, as expected from the theoretical charge profile for the battery shown in Fig. 1.

At higher SoC, the battery is less able to follow the setpoints as requested. These charge constraints are due to the battery chemistry and the constant voltage charging method utilized by the controller. The difference between the setpoint and the output during discharging (up-regulation) show that up-regulation has better accuracy across the different SoCs. One limitation of note is that, the battery does not respond to setpoints between –30 kW

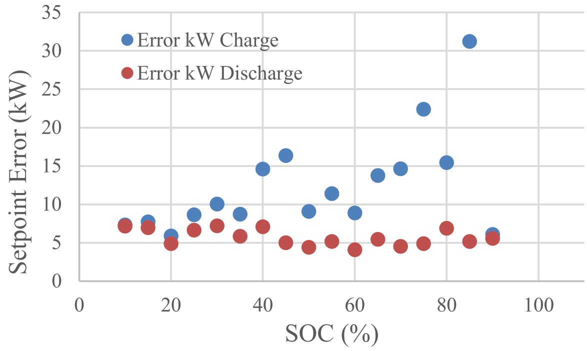

Fig. 10. State of charge vs. setpoint error during charging (down-regulation) and discharging (up-regulation).

and 30 kW; when the setpoint is in this range the battery has a real power of 0 kW.

July 2015 had the lowest monthly wind production at the Institute's site in recent years, with a capacity factor of 26.9% and 56.6% of the month had wind above 1 MW. Although use of energy storage as an ancillary service should not depend upon any constraints, normal AGC was constrained to when there was sufficient wind power to reduce demand charges from the local utility as discussed in Section III. When there was insufficient wind, the battery operated either in discharge only or idle mode, depending on the SoC of the battery. This constraint significantly reduced the time in which the battery was able to operate in normal mode. Repeating the experiment in multiple months with different wind profiles could reveal the relationship of idle time to the wind production. The chronological sequence of changes in the setpoints as well as the overlap of the changes in the setpoints with low wind periods will affect idle time.

There were several constraints while the battery was providing regulation. Firstly, the battery did not accept negative setpoints during low wind periods or if the SoC was above 90%. Secondly, the battery did not accept positive setpoints when the SoC was below 10%. Finally, as the battery's SoC increased, its ability to accurately match setpoints near –1000 kW decreased due to the charge profile constraints discussed earlier.

Although the maintenance cycle prevents GE Durathon's battery from performing AGC, the start time can be controlled and it can be interrupted if the battery is required for another purpose. As it happens on a predictable schedule, and all systems require maintenance and offline periods, and many generators are involved in AGC, this should not be seen as a major limitation.

A doughnut chart in Fig. 11 shows the time breakdown during the test period in July 2015. As noted in Fig. 11 the battery was able to perform normal AGC for 47% of total hours of operation. During 10% of the total hours, the battery was unable to perform AGC due to the maintenance cycle. Additionally, 25% of the time there was no wind and the SoC was below 10% so the BESS went into its idle state. One percent of the time was lost due to data error and SCADA communication errors. Overall, some form of AGC was operated for 64% of the 29 days.

The performance score (3) was calculated for each hour of the 29 days from the precision score, delay score, and accuracy

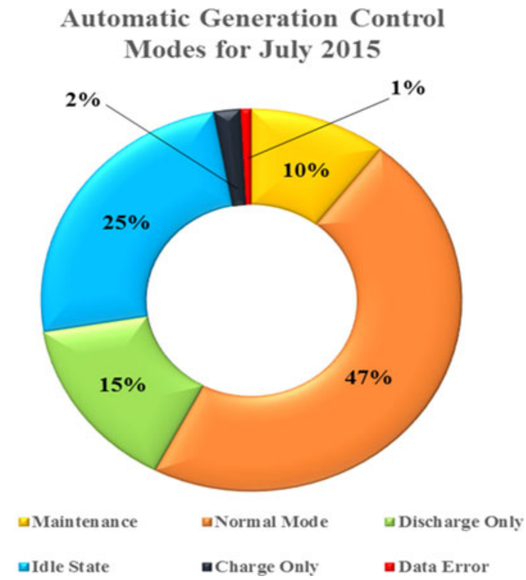

Fig. 11. Time spent in each battery operation mode in automatic generation control.

TABLE II
PJM Decay, Accuracy, Precision and Performance Scores for Each Percentage of Hour Providing AGC

Percentage of hour providing AGC	Hours in trial period	PJM Delay Score	PJM Accuracy Score	PJM Precision Score	PJM Performance Score
0%	256	49.1%	23.0%	29.6%	33.9%
1-33%	46	52.3%	30.3%	33.3%	38.6%
33-66%	89	90.8%	77.7%	63.9%	77.5%
66-99%	94	96.4%	91.0%	85.3%	90.9%
100%	211	96.4%	93.8%	89.5%	93.2%

score, as defined in (4), (5), and (6), based on the performance score template from PJM [21], [22]. The scores for each percentage of hour providing AGC are shown in Table II. Note that even when the battery is not performing AGC the scores are non-zero due to AGC signals and the BESS real power being similar some of the time, coincidentally. During periods where the battery is providing full AGC, which was 211 of the 696 total hours, the performance score is 93.2%. This is much higher than the performance scores reported for coal, gas, and hydro, which range from 67.4% to 85.6% [23]. This improvement is due to the rapid ramp speeds and excellent accuracy of the BESS. The –30 kW offset that was used in this work to account for efficiency losses of the battery decreased the accuracy, but meant the storage system did not need to take time to recharge as required in the Xu control strategy [9]. The AC/AC efficiency of the energy storage performing AGC was 76% in the study period, as shown in Table III. The manufacturer's efficiency for a round trip cycle is 85%. The lower operational efficiency has a variety of explanations including the large amount of time in idle state, where the battery used power to remain at its 280°C operating temperature. Charging and discharging the battery more frequently would increase the efficiency, but would also increase the battery's net loss. The availability of the battery for the study period was 98.9% due to one of the hundred modules

TABLE III
ENERGY IN AND OUT AND BATTERY EFFICIENCY FOR THE PERIOD OF STUDY

Energy In	Energy Out	Efficiency
54,723 kWh	41,675 kWh	76.2%

being offline for the entire month and one module being offline for a short period on July 7th. Counting the maintenance mode periods as unavailable lowers the availability to 92.5% for the period under study.

Based on PJM pricing for July 2015, for the 29 days of July over which the test was performed, a perfectly acting AGC source would have received USD 19,475, with 20% coming from the performance payment and the other 80% coming from the capability price [see (1)]. This value represents the ideal storage system that offers 1 MW of regulation and follows the signal with 100% accuracy. July's reg. D average of USD 28.0 MW is below the 2015 reg. D average of USD 36.2/MW, but above the reg. D 2016 average of USD 17.3/MW.

Assuming the battery is paid for hours when it provides AGC for at least half of the hour limits the battery to 342 of the total 696 hours. In these periods, the average capability price credit was USD 18.07, the average PJM performance was 91.1%, the average performance price was USD 2.20, and the average mileage ratio was 2.81. Summing the credits for each hour gives USD 9,037 over the 29 day test period.

Generalizing the results to a system that was independent of the wind power limitation, would allow the storage system to provide AGC for 90% of the study period (10% of the study period is the required weekly maintenance cycles). Using the same performance score, as recorded by the test storage system, this would give a payment of USD 16,363 over the 29 days. Eliminating the maintenance cycle would improve the financial performance by around USD 2,000.

The energy cost due to the inefficiency of the inverter/battery in the study period is USD 800 as calculated using the wholesale market price of the wind power used in this study. Assuming a lifetime of 4,500 cycles at 80% depth of discharge, July's usage corresponds to 26 cycles or 0.58% of the batteries' lifetime. Using the clock time of 29 days of the ten year lifetime estimated by the manufacturer calculates that 0.79% of the batteries' life has been expended. Taking the larger of these two values the depreciation of, the capital cost of the USD 2.3 million dollar BESS would be USD 18,200 for the 29 day study.

This experiment allowed for a storage system to be tested within a Wind R&D Park to calculate the real efficiency and accuracy of the system under test conditions. It highlighted the fast and precise response of the storage system while illuminating the charge rate limitation. Results were similar to expectations, although the amount of time in idle mode due to low wind conditions was surprising. The resulting decrease in efficiency was in line with expectation for the length of time in idle mode.

Another surprise during the experiment was that the battery could charge at rates significantly higher than the theoretical rate for short periods of time (<1 minute), until the battery would limit the charge rate to near the theoretical rate. In Fig. 12 the maximum charge rate (minimum power) is shown as a function of SoC. Additionally the average power is shown when the battery is automatically limiting the SoC. These are periods during AGC when the power and the setpoint are significantly different. The error bars give the standard deviation of these periods. Note that the battery performed better than expected at high SoC and worse than expected at low SoC. This, along with the average error shown in Fig. 10, give the main reason for the less than perfect performance. During up-regulation the maximum AC output was 966 kW (1000 kW DC), there was no additional limitations in the 10% to 90% SoC range.

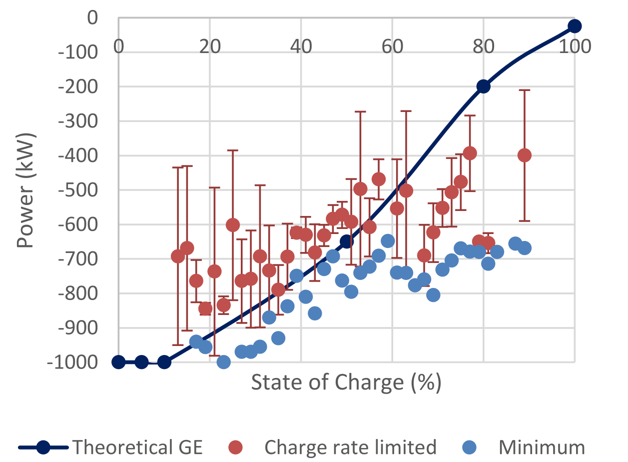

Fig. 12. Theoretical charge rates, average charge rate limited and minimum power as a function of SoC.

V. CONCLUSION

Although there were several limitations during the AGC, both self-imposed and technologically imposed, the battery performed well, and was able to carry out some mode of AGC 64% of the time. Utilizing PJM's score template showed that the 29 day long average performance score is 65% and during AGC, increased to 93%. This real-world analysis shows that batteries are fast response devices that can perform AGC.

This analysis demonstrates that there is value in performing both simulations and grid-connected battery operation. While simulations can show the ideal potential of a battery energy storage system, a grid-connected battery operation addresses realities such as maintenance cycles, reduced efficiency, reduced availability, charge rate limitations, and observing a higher charge rate than theoretically specified.

Including energy costs and degradation, the cost of utilizing the battery in this manner for 29 days was USD 19,000. With the potential income using the storage system, from behind the meter of a wind park, being USD 9,000, utilizing it with the restrictions given in this paper is clearly less than ideal. Creating a tariff scheme for storage systems that does not have a demand charge would allow independent storage units to be deployed on the network.

VI. Future Directions

Demonstrations of AGC should continue, offering less than the full power, i.e. 500 kW rather than 1 MW to reduce charge limitations and improve the accuracy of the storage system. Additionally, this would allow stacked services, with time-shifting being stacked simultaneously with AGC. While this work uses historical PJM signals, using live signals from the local balancing authority would allow a more realistic analysis and comparison with other generators on the network. Finally, the AGC should not depend upon the wind conditions, so a different tariff scheme for storage systems should be introduced when it is providing ancillary services.

Energy storage has the capability of providing various services such as AGC, time-shifting, and islanding, which are all potential grid applications. As more energy storage systems reliably demonstrate grid applications, utilities and system operators should see their value and more markets for their services will develop. Moreover, demonstrations of using a battery is important for the future electricity grid as conventional fossil fuel generators are displaced and retired.

Appendix

RTAC- Real Time Automation Controller
SCADA- Supervisory Control and Data Acquisition
AGC- Automatic Generation Control
PJM- Pennsylvania New Jersey Maryland Interconnection
ACE- Balancing Area Control Error

References

[1] N. S. Pearre and L. G. Swan, "Technoeconomic feasibility of grid storage: Mapping electrical services and energy storage technologies," *Appl. Energy*, vol. 137, pp. 501–510, 2015.

[2] Y. C. Zhang, V. Gevorgian, E. Ela, V. Singhvi, and P. Pourbeik, "Role of wind power in primary frequency response of an interconnection," presented at the Int. Workshop Large-Scale Integr. Wind Power Power Syst. Transm. Netw. Offshore Wind Power Plants, London, U.K., 2013.

[3] P. Denholm *et al.*, "The value of energy storage for grid applications," *Contract*, vol. 303, pp. 275–3000, 2013.

[4] D. Kottick, M. Blau, and D. Edelstein, "Battery energy storage for frequency regulation in an island power system," *IEEE Trans. Energy Convers.*, vol. 8, no. 3, pp. 455–459, Sep. 1993.

[5] E. Ela *et al.*, "Active power controls from wind power: Bridging the gaps," 2014. [Online]. Available: http://www.nrel.gov/docs/fy14osti/60574.pdf

[6] California Energy Storage Alliance, "Energy Storage—A Cheaper, faster cleaner alternative to conventional frequency regulation," 2011. [Online]. Available: https://www.ice-energy.com/wp-content/uploads/2016/04/cesa_energy_storage_for_frequency_regulation.pdf

[7] N. Miller, M. Shao, S. Pajic, and R. D'Aquila, "Eastern frequency response study," *Contract*, vol. 303, pp. 275–3000, 2013.

[8] N. Miller, M. Shao, S. Pajic, and R. D'Aquila, "Western wind and solar integration study phase 3—Frequency response and transient stability," 2014. [Online]. Available: http://www.nrel.gov/docs/fy15osti/62906.pdf

[9] B. Xu, A. Oudalov, J. Poland, A. Ulbig, and G. Andersson, "BESS control strategies for participating in grid frequency regulation," *Preprints 19th World Cong. Int. Fed. Autom. Control*, Cape Town, South Africa, 2014.

[10] O. Leitermann, "Energy storage for frequency regulation on the electric grid," Massachusetts Inst. Technol., Cambridge, MA, USA, 2012. [Online]. Available: http://www.ecoult.com/case-studies/pjm-pa-usa-frequency-regulation-services/

[11] ecoult. "Frequency regulation services: Ecoult grid energy storage and PJM interconnection (Pennsylvania, United States)." 2011. [Online]. Available: http://www.ecoult.com/case-studies/pjm-pa-usa-frequency-regulation-services/

[12] B. Gully, "Review of testing on 1MW lithium-ion battery at Reese Technology Center," in *Proc. EESAT Tech. Conf.*, Portland, OR, USA, 2015, pp. 1–15.

[13] M. Del Castillo, G. P. Lim, Y. Yoon, and B. Chang, "Application of frequency regulation control on the 4 MW/8 MWh battery energy storage system (BESS) in Jeju Island, Republic of Korea," *J. Energy Power Sources*, vol. 1, no. 6, pp. 287–295, 2014.

[14] A. A. Akhil *et al.*, "DOE/EPRI 2013 electricity storage handbook in collaboration with NRECA," Sandia Nat. Lab., Albuquerque, NM, USA, 2013.

[15] O. Mégel, J. L. Mathieu, and G. Andersson, "Scheduling distributed energy storage units to provide multiple services under forecast error," *Int. J. Electr. Power Energy Syst.*, vol. 72, pp. 48–57, 2015.

[16] G. E. Company, "Durathon batteries," Jul. 20, 2012.

[17] S. C. Electric, "S&C smart grid SMS storage management system," 2010. [Online]. Available: http://www.sandc.com/edocs_pdfs/EDOC_063209.pdf

[18] F. Chumbiauca, "RTAC system performance," Schweitzer Eng. Lab., Inc., Pullman, WA, USA, White Paper, 2011.

[19] D. Watson, T. Chakraborty, and M. Rodgers, "The need for SCADA communication in a wind R&D park," *Sustain. Energy Technol. Assess.*, vol. 11, pp. 65–70, 2015.

[20] GE Energy durathon DC system technical specifications—MWh series, 2014. [Online]. Available: https://renewables.gepower.com/content/dam/gepower-renewables/global/en-US/documents/Durathon-DCMWh-Spec-Sheet-GEA-988123002A.pdf

[21] S. Benner, "Performance score template," PJM, Norristown, PA, USA, 2014.

[22] C. Pilong, "PJM manual 12: Balancing operation," PJM, Norristown, PA, USA, Apr. 2016.

[23] A. Grewal, M. Dupos-Phillips,M. Wrinch, and D. Jang, "Regulating reserve performance assessment for the Alberta electric system operator: Project summary," Nat. Res. Council Canada, Energy, Mining Environ., Ottawa, ON, Canada, Tech. Rep. NRC-EME-55756, 2016.

Tapabrata Chakraborty received the Bachelor's degree in electrical engineering from St. Thomas' College of Engineering and Technology, Calcutta, WB, India, in 2011, and the Master's degree in electronics systems engineering from the University of Regina, Regina, SK, Canada, in 2016. His interests are mainly but not limited to power system analysis, grid protection and reliability, synchronous machines, and renewable energy.

David Watson received the B.S. degree in physics from Mount Allison University, Sackville, NB, Canada. He also has a European Master's degree in renewable energy from Loughborough University, Loughborough, U.K. He worked for CIRCE, a research center in Spain, where he was responsible for developing a microgrid with load response and a control system to integrate advanced grid protections in pre-existing wind farms. His main responsibility at the Institute is the battery storage system which is used for the integration of wind energy into the electricity network.

Marianne Rodgers received the B.S. degree from St. Francis Xavier University, Antigonish, NS, Canada, and the Ph.D. degree from the Simon Fraser University, Burnaby, BC, Canada. While completing her doctoral studies, she worked with the National Research Council, Vancouver, BC. Following her graduation, she worked as a Research Professor with the Florida Solar Energy Center, Cocoa, FL, USA, where she performed research on several types of alternative energies, including fuel cells, batteries, and photovoltaics. She is currently the Scientific Director of the Wind Energy Institute of Canada, North Cape, PE, Canada, where she focuses on research that advances the development of wind energy across Canada.